

# Tracking of Tagged MR Images by Bayesian Analysis of a Network of Quads

Delman Lee\*, John T. Kent\* and Kanti V. Mardia\*

## Abstract

Automatic tracking of tagged MR image sequences is done frame-by-frame. For each frame, a quadrilateral (quad) detector is run over the image to give a set of “potential quads”. A likelihood function is specified for the detection of potential quads from an image. Quads are picked from the set of potential quads to form a “quilt”. Quads are present where a grid structure is apparent in the image. A prior is specified to govern how the quads should be joined up to form the quilt. The prior for the quilt (i) encourages quads to be close to their positions predicted from the last frame, (ii) encourages neighbouring quads to be close to each other, (iii) discourages intersecting quads, (iv) avoids “tears” in the quilt, and (v) encourages connectedness of quads. With the likelihood and prior densities, a Bayesian analysis is carried out using the Markov Chain Monte Carlo method on the posterior density to give an estimate of the posterior mode.

---

\*Email: {delman, john, sta6kvm}@amsta.leeds.ac.uk Post: Department of Statistics, University of Leeds, Leeds, LS2 9JT, U.K..

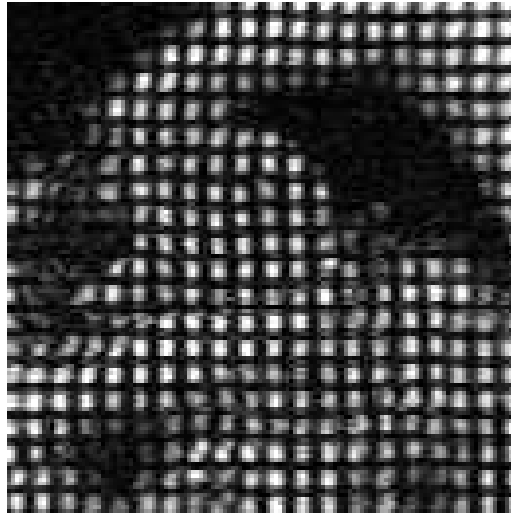


Figure 1: A typical first frame of an MRI-SPAMM image sequence of the left ventricle (short-axis).

## 1 Introduction

A non-invasive method for monitoring the deformation of the heart wall is by tagged Magnetic Resonance Imaging (MRI), often called MRI-SPAMM (SPAtial Modulation of Magnetization) images [1]. A typical MRI-SPAMM initial frame of the left ventricle is shown in Fig. 1. The dark lines forming the grid are “tagged” to the material points (in planes perpendicular to the imaging plane), and as such follow the material points through time. In subsequent time frames, the contrast between the tagged and non-tagged materials decreases, and, furthermore, lines tagged to fluid material (e.g. blood) disappear. Tracking the grid through time provides deformation information that is useful for diagnosis of certain heart diseases, e.g. ischemia. This paper focuses on the issue of tracking of the tagged grid to establish point correspondence through time.

Many past tracking techniques for MRI-SPAMM images [2–6] follow the dark tagged lines through time with deformable splines, e.g. *snakes* [7]. A spline is influenced by two forces — internal and external. The internal force maintains the smoothness of the spline, while the external force pulls the spline to features (e.g. edges or grooves) in the image. In this paper we investigate the dual problem of tracking the network of (approximate) quadrilaterals formed by the grid lines, rather than the lines themselves. *Quadrilateral* will hereafter be shortened to *quad*.

Tracking of tagged MR image sequences is done frame-by-frame. For each frame, a quadrilateral (quad) detector is run over the image to give a set of “potential quads”. A likelihood function is specified for the detection of potential quads from an image. Quads are picked from the set of potential quads to form a “quilt”. The quads in the quilt are connected by a square graph structure and can be either alive or dead at each time frame. For a particular frame, live quads account for tagged materials, for example heart wall, that are visible, and dead quads account for tagged materials whose structure is no longer apparent, for example blood. A prior is specified to govern how the quads should be joined up, it (i) encourages quads to be close to their positions predicted from the last frame, (ii) encourages neighbouring quads to be close to each other, (iii) discourages intersecting quads, (iv) avoids “tears” in the quilt, and (v) encourages the connectedness of the live quads.

Having specified a posterior density in terms of a likelihood and a prior, one can employ fast deterministic local searches to give a local maximum of the density. However, we have chosen to use stochastic optimization based on Markov chain Monte Carlo (MCMC) methods (see e.g. [8]) to avoid the solution being trapped in minor subsidiary modes of a “bumpy” posterior.

Section 2 discusses the principles behind the method, and sections 3 and 4 detail the implementation. We discuss how to summarize the samples from our MCMC in section 5, and present some results in section 6.

## 2 Principles of the Method

The tracking is done in a frame-by-frame manner. For each successive frame, we use a Bayesian strategy to infer about “model”  $x$  and “unobserved data”  $\mu$  from “observed data”  $y$ , where  $x$ ,  $\mu$  and  $y$  are detailed below. Let  $f(y, \mu|x)$  and  $f(x)$  denote the likelihood function (§ 2.3) and prior density (§ 2.2), respectively. Information about the model and the unobserved data are contained in the posterior distribution  $f(x, \mu|y)$  given by

$$f(x, \mu|y) \propto f(y, \mu|x)f(x). \quad (1)$$

Inference about the posterior density is done by sampling using the Markov Chain Monte Carlo (MCMC) method (§ 4) [8].

Let a quad be represented by  $q_i=(c_i, v_i)$ , where  $c_i$  is the centre of the quad, and  $v_i$  is the set of the four vertices of the quad. The centre of the quad  $c_i$  is not strictly necessary, but it is kept in the representation for convenience. For each frame, the image is pre-processed by a quad detector to give a set of  $P$  “potential quads”  $\check{q}=\{\check{q}_p\}_{p=1}^P$ ,  $\check{q}_p=(\check{c}_p, \check{v}_p)$  and their “certainties”  $e=\{e_p\}_{p=1}^P$ . The quad detection (§3) is susceptible to noise, and a measure of certainty  $0 < e_p < 1$  is calculated to assess how sure we are of the existence of the quad  $\check{q}_p$ . The set of potential quads and their certainties  $y=(\check{q}, e)$  is our observed data. The goal is to find a subset of the potential quads from our observation  $y$  to form a “quilt” representing non-fluid materials in the image, e.g. the heart muscle. The model  $x$  on the quilt is discussed in § 2.2.

### 2.1 Quilt Representation

Let  $\mathcal{G}$  be an  $n$ -node undirected graph associated with a subset of a 2D square lattice. Nodes in the graph are indexed by  $i = (i_1, i_2) \in \mathbb{Z}^2$ , and are connected with 8-adjacency. The extent of the square lattice is specified by the user in the first frame. In subsequent frames,  $\mathcal{G}$  is the output from processing of the previous frame.

Once  $\mathcal{G}$  is specified at a time frame, the components of our model  $x$  are (i) the maximum number of quads,  $n$ , that can make up a quilt, (ii) the positions and vertices of the quads,  $q=\{q_i\}_{i \in \mathcal{G}}$ , and (iii) the statuses, dead ( $s_i=0$ ) or alive ( $s_i=1$ ), of the quads,  $s=\{s_i\}_{i \in \mathcal{G}}$ . Two quads  $q_i$  and  $q_j$  are neighbours if the nodes  $i$  and  $j$  share an edge in the graph  $\mathcal{G}$ , and we write  $i \sim j$  in such a case.

The set of live quads in  $x$  forms the “fabric” of the quilt, while the set of dead quads corresponds to “holes” in the quilt. Let  $\mathcal{L}$  denote the set of indices of the live quads in  $x$ , and  $n_{\text{alive}}=\sum_{i \in \mathcal{G}} s_i$  the number of live quads. Thus the model  $x=(q, s)$  (leaving out the underlying graph structure for convenience) defines a quilt in a certain region.

## 2.2 Quilt Prior

In this section, we discuss the prior for the quilt  $x=(q, s)$ :

$$f(x) = f(q, s) = f(q)f(s) \quad (2)$$

where  $q$  and  $s$  are assumed to be independent. For the prior on the status, we assume a truncated Ising model:

$$f(s) \propto \exp \left( \alpha \sum_{i \in \mathcal{G}} s_i + \beta \sum_{i \sim j} s_i s_j \right) \mathbb{I}[s \in \mathcal{S}] \quad (3)$$

where  $s_i \in \{0, 1\}$ ,  $\mathbb{I}[\cdot]$  is the indicator function, and  $\mathcal{S} \subset \{0, 1\}^n$  is the set of configurations such that the live quads form one connected component. With  $\beta > 0$ , the second term in the exponent of Eq. (3) encourages the interconnectedness of the live quads, and discourages a checkerboard pattern for  $s$ . For the simulations in § 6, we have chosen  $\alpha = -4$ , and  $\beta = 1$ .

For the prior on the quads, we assume

$$f(q) \propto \exp \left( -\frac{1}{2} \sum_{i \in \mathcal{G}} \Delta_i^T R_i \Delta_i \right) \quad (4.1)$$

$$\cdot \exp \left( -\frac{1}{2} \sum_{i \sim j} \Delta_j^T S_{ij} \Delta_i \right) \quad (4.2)$$

$$\cdot \prod_{\substack{i \sim j, k \\ j \neq k}} \mathbb{I}[\|\angle(c_j, c_i, c_k) - \theta_{jik}\|_{2\pi} < \phi] \quad (4.3)$$

$$\cdot \exp \left( -\gamma \sum_{i, j \in \mathcal{G}} q_i \cap q_j \right). \quad (4.4)$$

Based on information from previous frames, we have a prediction of where the quads  $q$  are in the current frame. i.e. we have a set of  $n$  predicted positions  $\hat{c} = \{\hat{c}_i\}_{i \in \mathcal{G}}$  and a set of  $n$   $2 \times 2$  covariance matrices  $\Sigma_i$  of the prediction error. Let  $\Delta_i = c_i - \hat{c}_i$  be the deviation from the predicted position of the centre of the quad  $i$ . The term (4.1) enforces our belief that the positions of the quads are not too far away from their predicted values, while the interaction term (4.2) encourages departures from predicted positions to be similar for neighbouring quads. Note that the matrices  $R_i$  (positive definite) and  $S_{ij}$  (negative definite) are chosen such that the covariance matrix of the resultant quadratic form when terms (4.1) and (4.2) are combined is positive definite.

Let  $\|\theta\|_{2\pi} = |\theta + 2\pi k|$ , where the integer  $k$  is chosen such that  $-\pi < \theta + 2\pi k < \pi$ . Let  $\angle(c_j, c_i, c_k)$  denote the angle formed by the three points  $(c_j, c_i, c_k)$  with  $c_i$  at the apex, and  $\theta_{jik}$  be the expected angle formed by the centres of the three quads  $(q_j, q_i, q_k)$  with  $q_i$  at the apex.  $\phi$  is the allowed deviation from the expected angle  $\theta_{jik}$ . For an 8-adjacency graph, we chose  $\phi = \pi/4$ . The term (4.3) aims to preserve the regularity of the quilt, avoiding tears, see Fig. 2.

Let  $q_i \cap q_j$  denote the area of intersection of the interior of the two quads  $q_i$  and  $q_j$ . With  $\gamma > 0$ , the term (4.4) penalizes against intersecting quads, and allows quads to be packed more closely in regions of small quads. Term (4.4) is the only term in (4) which depends on the vertices of the quads. For the simulations in § 6, we have chosen  $\gamma = 1$ .

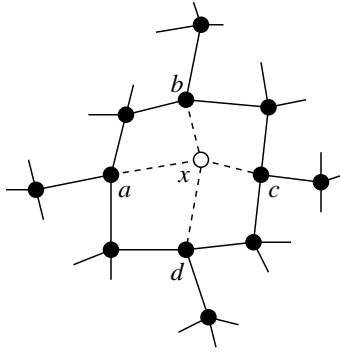


Figure 2: Illustration of the term (4.3) in the prior for a 4-adjacency graph. For each node  $x$ , term (4.3) ensures that the angles  $\angle(a, x, b)$ ,  $\angle(a, x, c)$ ,  $\angle(a, x, d)$ ,  $\angle(b, x, c)$ ,  $\angle(b, x, d)$  and  $\angle(c, x, e)$  are within their expected ranges. For example,  $\angle(a, x, b)$  should be within  $\pi/2 \pm \pi/4$ .

Note that the prior  $f(x)$  has the Markov property with neighbourhoods up to second order, and thus allowing efficient implementation for the MCMC simulation in § 4.

### 2.3 Incomplete Data and Likelihood

In this section we specify a probability density on how the data are generated from a quilt. Consider a hypothetical quad detector which takes a quilt  $x$  as input and generates a list of  $P$  potential quads  $\check{q}$ , their certainties  $e$ , and a mapping  $\mu(\cdot)$ . The function  $\mu(\cdot)$  maps  $\mathcal{G}$  to  $\{0, 1, \dots, P\}$ . The mapping describes which potential quad in  $\check{q}$  corresponds to which model quad in  $x$ . Further  $\mu(i)=0$  means that quad  $i$  does not correspond to any potential quads in  $\check{q}$ . Let  $z(\mu)$  be the number of zeros in  $\{\mu(i)\}_{i \in \mathcal{G}}$ . We assume that all live quads in  $x$  are detected exactly once, i.e. the mapping from the set  $\mathcal{L} = \{i : \mu(i) > 0\}$  to  $\{1, \dots, P\}$  is injective.

The actual quad detector takes an image as input and generates the potential quads  $\check{q}$  and their certainties  $e$ . The mapping  $\mu$  is unobserved and represents missing data, while  $y = (\check{q}, e)$  are the observed, incomplete data.

To specify the likelihood for  $(y, \mu)$  given  $x$ , we need to answer the question: given a quilt  $x$ , what is the probability of the hypothetical quad detector generating potential quads  $\check{q}$ , certainties  $e$ , and mapping  $\mu(\cdot)$ ? We model our likelihood function  $f(y, \mu|x)$  as a product of three factors:

$$f(y, \mu|x) = f(\check{q}, e, \mu|x) = f(\check{q}|\mu, x)f(e|\mu, x)f(\mu|x) \quad (5)$$

where  $\check{q}$  and  $e$  are assumed to be independent given  $\mu$  and  $x$ .

Given the quilt  $x$ , we place a uniform weight on all permissible mappings  $\mu$ . There are  $P!/(P - n_{\text{alive}})!$  possibilities, and thus  $\mu$  has a discrete distribution:

$$f(\mu|x) = \begin{cases} (P - n_{\text{alive}})!/P! & \text{if } z(\mu) = P - n_{\text{alive}}, \\ 0 & \text{otherwise.} \end{cases} \quad (6)$$

Given the quilt  $x$  and the mapping  $\mu$ , the potential quad that corresponds to a live quad should have a certainty close to unity, and one that does not correspond to any live quads should have a certainty

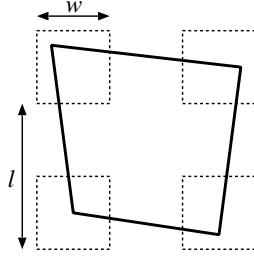


Figure 3: Quad template. Each vertex is allowed to be within a certain region relative to other vertices.

close to zero. We model these two cases with beta densities  $f(x)=x^2/3$  and  $f(x)=(1-x)^2/3$  for  $0 < x < 1$ , respectively. Assuming independence between the certainties of different potential quads, we have

$$f(e|\mu, x) = \frac{1}{3^P} \prod_{p \notin \mathcal{M}} (1 - e_p)^2 \prod_{p \in \mathcal{M}} e_p^2 \quad (7)$$

where  $\mathcal{M} = \{\mu(i) : i \in \mathcal{L}\}$  is the set of indices of potential quads corresponding to live model quads.

Finally, given the quilt  $x$  and the mapping  $\mu$ , the quad detector is assumed to detect all live quads in  $x$  precisely, and gives out  $P - n_{\text{alive}}$  artefactual potential quads. The artefactual potential quads are assumed to be uniformly distributed on the space of possible outputs of the quad detector. We denote the “volume” of such 8-dimensional space by  $AV$  (see § 3). We thus have

$$f(\check{q}|\mu, x) = \frac{1}{(AV)^{z(\mu)}} \prod_{i \in \mathcal{L}} \mathbb{I}[\check{q}_{\mu(i)} = q_i]. \quad (8)$$

Note that an artefactual potential quad  $\check{q}_i$  has a probability density on  $\mathbb{R}^8$  if  $s_i=0$ , and has a point mass if  $s_i=1$ .

We remark that the likelihood does not depend on the locations of dead quads in  $x$ . If we were to estimate  $x$  by maximum likelihood, then the dead quads would be unestimable. However, with the prior  $f(x)$ , the dead quads are estimable. The dead quads are kept in the model for technical reasons regarding detailed balance in the Markov chain we construct in § 4.

### 3 Quad Detector

We shall present the quad detector in a continuous setting. Appropriate discretization is required for implementation. Each frame is pre-processed by the quad detector to give a set of potential quad positions. We used the simple quad template shown in Fig. 3, where each vertex is allowed to be within a certain region relative to other vertices. The size  $w$  of the regions, and the distance  $l$  between regions are chosen to reflect the expected sizes of the quads in the image. The quad detector as implemented only detects rectangles that are close to a standard square, and thus only handles mild deformations (scale changes and rotations).

Let  $I(s)$ ,  $s \in \mathcal{A}$ , be a gray-scale image, where  $\mathcal{A}$  is a rectangular region of area  $A$ , and let  $u_+ = u$

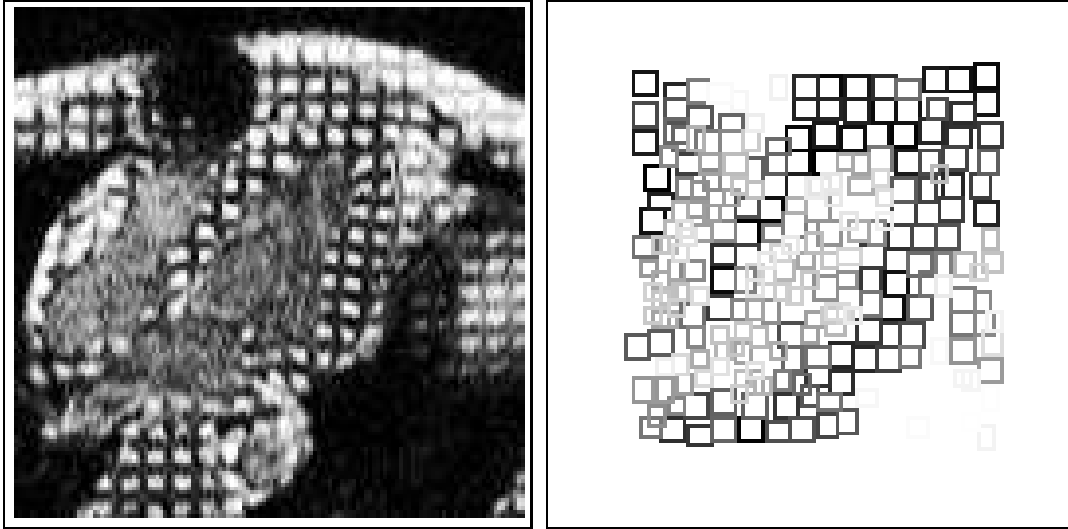


Figure 4: The right picture shows the potential quads generated by the quad detector on the left image. The darker the potential quad, the higher the certainty.

if  $u > 0$ , and  $u_+ = 0$  if  $u \leq 0$ . Define a template function

$$e(v) = \left[ \frac{1}{\int_{B'(v)} ds'} \int_{B'(v)} I(s') ds' - \frac{1}{\int_{B(v)} ds'} \int_{B(v)} I(s') ds' \right]_+ \quad (9)$$

where  $B(v)$  and  $B'(v)$  are, respectively, the boundary and interior of a quad with vertex set  $v$ . The template function  $e(v)$  calculates the image contrast between the interior and boundary of a quad.

Each quad is defined by a set of vertices  $v \in \mathbb{R}^8$ . Let  $\mathcal{V}(s)$  be the set of permissible template vertex sets whose centre of gravity is at  $s$ , this defines a 6-dimensional region in  $\mathbb{R}^8$ . Let  $V$  denote the ‘‘volume’’ of the set  $\mathcal{V}(s)$ . For each site  $s$  in the image, we maximize the template function  $e(v)$  over  $\mathcal{V}(s)$  to get  $e(v_{\max}(s))$ , where

$$v_{\max}(s) = \operatorname{argmax}_{v \in \mathcal{V}(s)} e(v). \quad (10)$$

The largest  $P$  local maxima of  $e(v_{\max}(s))$  over  $s \in \mathcal{A}$  are selected to give the set of potential quads  $\check{q} = \{\check{q}_1, \dots, \check{q}_P\}$  and their certainties  $e = \{e_1, \dots, e_P\}$ . Fig. 4 shows a sample output of the quad detector. For the simulations in § 6, we have chosen  $P = 2n$ .

## 4 Posterior Sampling

In order to gain information about the posterior, we used the MCMC method with a Metropolis-Hastings [9, 10] type algorithm that allows jumps between different dimensional spaces [11, 12]. The dimension changing aspect of our model comes from sites being alive or dead. The algorithm generates a Markov chain, whose stationary distribution is the posterior density  $f(x, \mu | y)$ . In this section, we describe the details of the algorithm.

At each MCMC iteration, the algorithm proposes one of four types of transitions: live-displacement, dead-displacement, birth and death. The four types of transitions are proposed with probabilities  $(1 -$

$p)/2$ ,  $(1 - p)/2$ ,  $p/2$ , and  $p/2$ , respectively. For each type of transition, a node  $i$  is chosen randomly from the feasible nodes, and new values for the component  $i$  of the quilt  $(q_i, s_i)$  and for the component  $i$  of the mapping  $\mu(i)$  are proposed with a certain probability. The proposed values are then accepted with a certain acceptance probability  $a$ .

It can be shown that the proposal distributions and acceptance probabilities described below for the four types of transitions satisfy detailed balance and the proposed Markov chain is ergodic (see e.g. [13]) with the desired stationary distribution.

### Live-Displacement Transition

For a live-displacement transition, one of the live nodes  $i$  is chosen with probability  $1/n_{\text{alive}}$ . The following move is then proposed for the node  $i$ :

$$q_i = \check{q}_p \rightarrow q_i = \check{q}_{p'} \quad ; \quad \mu(i) = p \rightarrow \mu(i) = p' . \quad (11)$$

The potential quad  $\check{q}_{p'}$  is drawn from the set of unpicked potential quads  $\mathcal{P}_\mu$  with probability  $H(\check{q}_{p'}|\mu, \check{c}_p)$ , where

$$H(\check{q}_{p'}|\mu, c_*) = \mathbb{I}[\check{q}_{p'} \in \mathcal{P}_\mu] \frac{\exp(-\|\check{c}_{p'} - c_*\|/\sigma_i)}{\sum_{\check{q}_r \in \mathcal{P}_\mu} \exp(-\|\check{c}_r - c_*\|/\sigma_i)} . \quad (12)$$

$H(\cdot)$  thus puts a higher probability on unpicked potential quads that are closer to the current position of  $q_i$ .  $\sigma_i^2$  is the maximum diagonal value of the covariance matrix  $\Sigma_i$  of the prediction error (§ 2.2). The acceptance probability of the proposed live-displacement of quad  $i$  is:

$$a[(x, \mu) \xrightarrow{ld} (x', \mu')] = \min \left[ 1, \frac{f(x', \mu'|y) H(\check{q}_p|\mu', \check{c}_{p'})}{f(x, \mu|y) H(\check{q}_{p'}|\mu, \check{c}_p)} \right] \quad (13)$$

where  $x'$  and  $\mu'$  are the quilt  $x$  and the mapping  $\mu$  updated with the proposed move of Eq. (11).

### Dead-Displacement Transition

For a dead-displacement transition, one of the dead nodes  $i$  is chosen with probability  $1/(P - n_{\text{alive}})$ . The following move is then proposed for node  $i$ :

$$q_i = q_* \rightarrow q_i = q'_* . \quad (14)$$

The proposed quad  $q'_*$  is a translation of  $q_*$ . The centre  $c'_*$  of  $q'_*$  is drawn from a Gaussian density

$$G(c'_*|c_*) = \frac{1}{2\pi\sigma_i^2} \exp\left(-\frac{\|c'_* - c_*\|^2}{2\sigma_i^2}\right) . \quad (15)$$

Because of the symmetry of the proposal distribution, the acceptance probability is simply the ratio of the posterior density:

$$a[(x, \mu) \xrightarrow{dd} (x', \mu)] = \min \left[ 1, \frac{f(x', \mu|y)}{f(x, \mu|y)} \right] \quad (16)$$

where  $x'$  is the quilt  $x$  updated with the proposed move of Eq. (14).

## Birth and Death Transitions

For a birth transition, one of the dead nodes  $i$  that is a neighbour of a live node is picked with probability  $1/n_{\text{periph}}$ , where  $n_{\text{periph}}$  is the number of dead nodes that are neighbours of a live one. The following move is then proposed for node  $i$ :

$$q_i = q_* \rightarrow q_i = \check{q}_{p'} \quad ; \quad s_i = 0 \rightarrow s_i = 1 \quad ; \quad \mu(i) = 0 \rightarrow \mu(i) = p' . \quad (17)$$

The potential quad  $\check{q}_{p'}$  is drawn from the set of unpicked potential quad  $\mathcal{P}_\mu$  with probability  $H(\check{q}_{p'}|\mu, c_*)$  of Eq. (12).

An articulation point of a connected graph is a node, whose removal would result in two separate connected components. For a death transition, one of the live nodes  $i$ , which is not an articulation point of the graph formed by the live quads, is picked with probability  $1/(n_{\text{alive}} - n_{\text{art}})$ , where  $n_{\text{art}}$  is the number of articulation points in the graph formed by the live quads. The following move is then proposed for node  $i$ :

$$q_i = \check{q}_{p'} \rightarrow q_i = q_* \quad ; \quad s_i = 1 \rightarrow s_i = 0 \quad ; \quad \mu(i) = p' \rightarrow \mu(i) = 0 . \quad (18)$$

The centre  $c_*$  of the quad  $q_*$  is drawn from the Gaussian density  $G(c_*|\check{c}_{p'})$  of Eq. (15), while the vertices of  $q_*$  are drawn uniformly from  $\mathcal{V}(c_*)$  (see § 3).

With  $x'$  being the quilt  $x$  updated with the proposed birth move of Eq. (17), define the ratio

$$r(x, x') = \frac{f(x', \mu'|y)}{f(x, \mu|y)} \frac{n_{\text{periph}}}{H(\check{q}_{p'}|\mu, c_*)} \frac{G(c_*|\check{c}_{p'})}{(n_{\text{alive}} - n_{\text{art}})V} . \quad (19)$$

The acceptance probabilities for birth and death proposals are:

$$a[(x, \mu) \xrightarrow{b} (x', \mu')] = \min[1, r(x, x')] \quad \text{and} \quad (20)$$

$$a[(x', \mu') \xrightarrow{d} (x, \mu)] = \min[1, 1/r(x, x')] . \quad (21)$$

## Chain Initialization

The Markov chain is initialized by the following procedure. Let  $x^{(t-1)} = (q^{(t-1)}, s^{(t-1)})$  be the estimated quilt from frame  $t-1$ . The graph  $\mathcal{G}^{(t)}$  for time frame  $t$  is formed by removing all the dead quads in the previous quilt model  $x^{(t-1)}$ , i.e.  $n^{(t)} = n_{\text{alive}}^{(t-1)}$ . The preliminary statuses of all the quads in  $x^{(t)}$  are set to dead. The positions of the quads at  $t-1$  become the predicted positions of the quads at  $t$ .

A greedy version of the Markov chain (similar to the Iterative Conditional Mode (ICM) method of [14]) is then run where only births with potential quads nearest to the predicted position of the nodes are proposed, and the proposed birth is accepted only if the posterior density is increased. The quilt from such a greedy Markov chain is the initial state of the full MCMC algorithm described in § 4.

## 5 Summary Statistics

The samples from the Markov chain are collected after a burn-in period. Given that we have a sequence of samples from the posterior distribution, how can we summarize our results? Summarizing the posterior by its mean comes immediately to mind. However, for the type of objects that we are dealing

with, there is no clear definition of a mean or variance. We propose to summarize the posterior by its “restricted” marginal modes.

For a fixed  $i \in \mathcal{G}$ , consider the histogram of the mapping  $\mu, h_{\mu(i)}(p), p \in \{0, 1, \dots, P\}$ , whose entry is the frequency that the  $p$ th potential quad is picked by quad  $i$  in the quilt. Picking a potential quad of 0 means that the quad is dead.

For all the nodes that have been alive for more than a certain percentage of iterations of the chain (10% in our simulations), rescale the histogram  $h_{\mu(i)}(p)$  to sum up to 1 for  $p \neq 0$ . We scan through the nodes according to the entropies of their rescaled histograms. Nodes with lower entropies are scanned first. For each scanned node  $i$ , the potential quad  $\check{q}_p$  is picked, where  $p$  is the mode of the rescaled histogram. Node  $i$  is then born if  $\check{q}_p$  is not already associated with a live node. After scanning through all the nodes, the live quads which form the largest single connected component is our estimate of the quilt for the current frame.

## 6 Results

Figs. 5 and 6 show the successful tracking of two nine-frames image sequences. Due to page limitations, only the last six frames are shown. For clarity, only the 4-adjacent edges of the graph are drawn. The nodes of the graph in the figures correspond to the centres of the quads. The tracking is done for a region of interest specified by the user. The results are for a MCMC simulation with 300 sweeps (1 sweep =  $n$  iterations), of which 100 are for burn-in. The tracking for the nine frames took 20mins and 5mins on an i486-133MHz and UltraSPARC-167MHz respectively. Note the successful tracking in Fig. 6 where there is a large region without quads. The effectiveness of the results can be best appreciated by a movie of the deformation, which will be presented in the talk.

## 7 Discussion

The algorithm assumes that the Markov chain has converged after a certain number of burn-in sweeps. In this paper, the number of burn-in sweeps is arrived at by inspection. Many convergence diagnostics have been proposed recently (see e.g. [15]) and should be incorporated into the algorithm. Related to the rate of convergence is the mixing property of the Markov chain. Our current algorithm proposes single-node transitions. Transition that updates a block of nodes at a time are being investigated to improve the mixing property of the Markov chain.

Because there is no substantial motion from frame to frame, using the estimated positions of quads from the previous frame as an initial estimate in the current frame works satisfactorily. If the inter-frame motion becomes severe, motion prediction should be incorporated in the algorithm. A plausible first attempt would be to treat the motion of each quad independently of others, and have a Kalman filter (with, say, a constant acceleration model) for the motion of each quad.

The paper has only dealt with the problem of tracking the tagged grid. The next step is to deduce the full 3D motion of the left ventricle. With current MRI-SPAMM techniques, motion perpendicular to the acquisition plane (through-plane motion) are not accounted for. Image sequences acquired at orthogonal planes are required to resolve the 3D motion (see e.g. [16]).

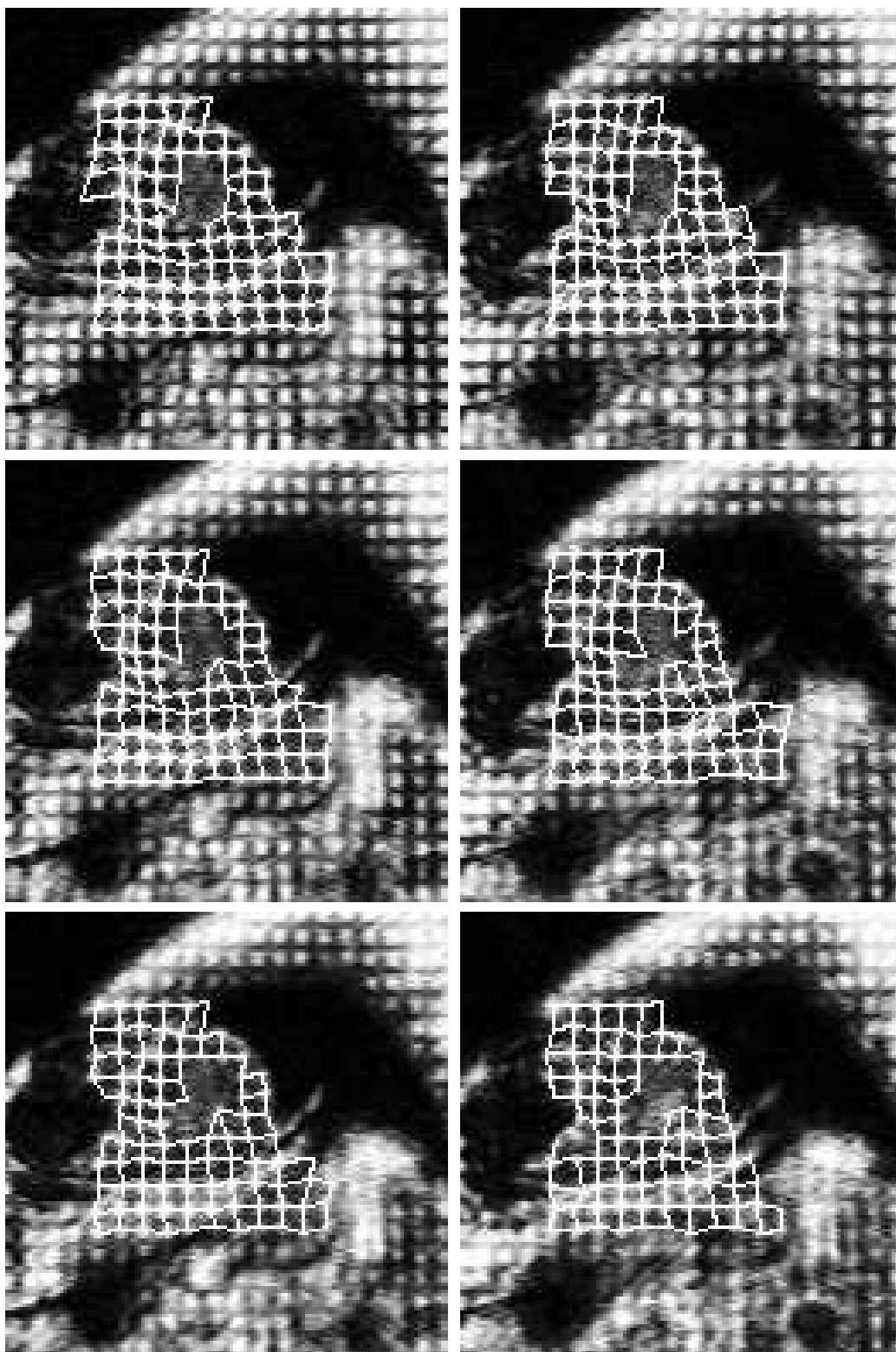


Figure 5: The graph structure of the network of quads for the last six frames of a nine-frames short-axis sequence of the left ventricle. For clarity, only the 4-adjacent edges of the graph are drawn.

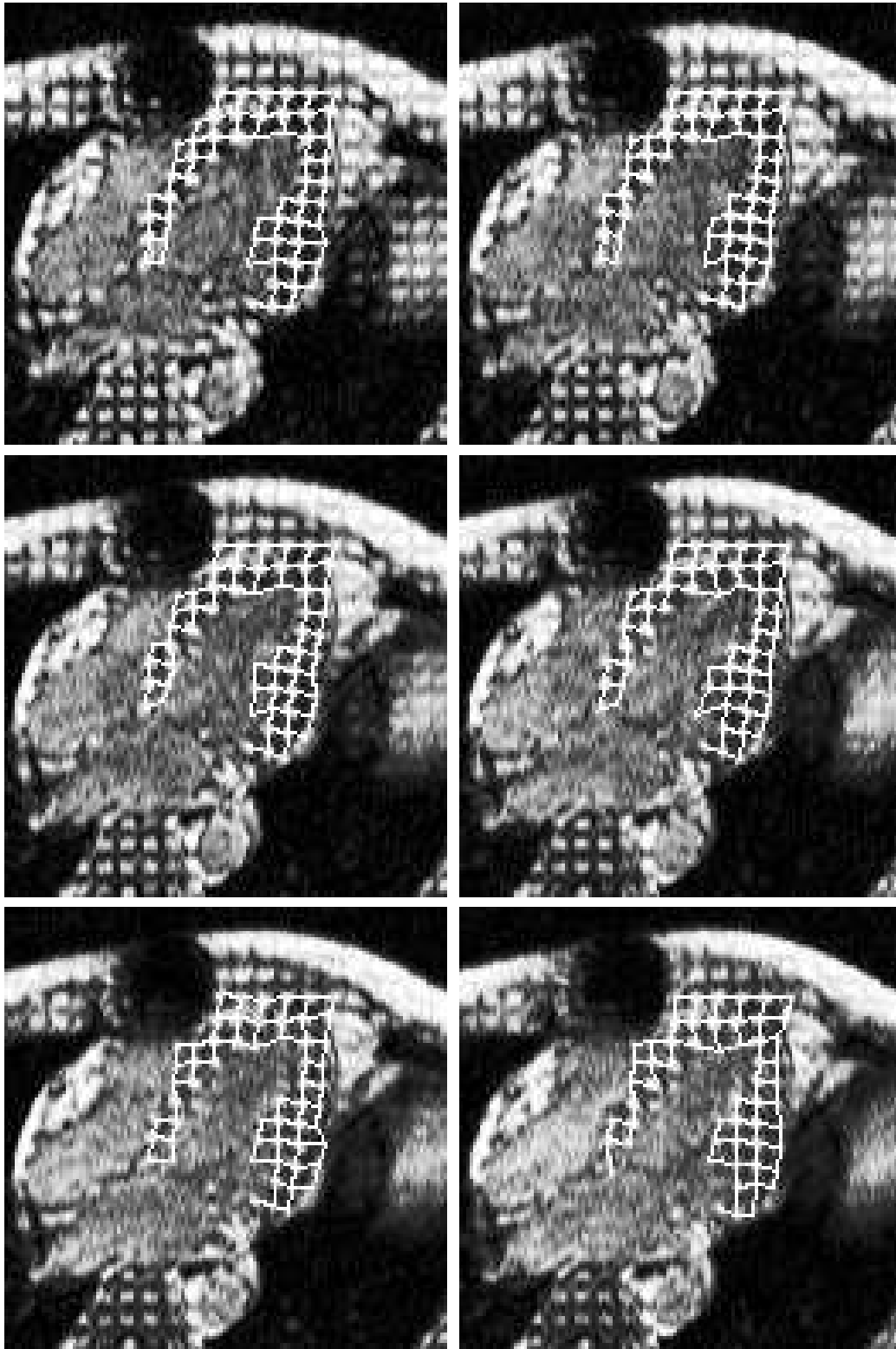


Figure 6: The graph structure of the network of quads for the last six frames of a nine-frames long-axis sequence of the left ventricle. For clarity, only the 4-adjacent edges of the graph are drawn.

## 8 Acknowledgment

The work is supported under the EPSRC Stochastic Modelling in Science and Technology programme. We would like to thank Liz Berry, Bill Crum, John Ridgway and U. Sivananthan for useful discussions and for providing us with the data set.

## References

- [1] L. Axel and L. Dougherty, “Heart wall motion: Improved method of spatial modulation of magnetization for MR imaging,” *Radiology*, vol. 172, pp. 349–350, 1989.
- [2] M. Guttman, J. Prince, and E. McVeigh, “Tag and contour detection in tagged MR images of the left ventricle,” *IEEE Transactions on Medical Imaging*, vol. 13, pp. 74–88, Mar 1994.
- [3] S. Kumar and D. Goldgof, “Automatic tracking of SPAMM grid and the estimation of deformation parameters from cardiac MR images,” *IEEE Transactions on Medical Imaging*, vol. 13, pp. 122–132, Mar 1994.
- [4] A. Young, D. Kraitchman, L. Dougherty, and L. Axel, “Tracking and finite element analysis of stripe deformation in magnetic resonance tagging,” *IEEE Transactions on Medical Imaging*, vol. 14, no. 3, pp. 413–421, 1995.
- [5] D. Kraitchman, A. Young, C. Chang, and L. Axel, “Semi-automatic tracking of myocardial motion in MR-tagged images,” *IEEE Transactions on Medical Imaging*, vol. 14, no. 3, pp. 422–433, 1995.
- [6] P. Radeva, A. Amini, J. Huang, and E. Martí, “Deformable B-solids and implicit snakes for localization and tracking of SPAMM MRI-data,” in *Proceedings of the IEEE Workshop on Mathematical Methods in Biomedical Image Analysis*, pp. 192–201, June 1996.
- [7] M. Kass, A. Witkin, and D. Terzopoulos, “Snakes: Active contour models,” *International Journal of Computer Vision*, vol. 1, no. 4, pp. 321–331, 1988.
- [8] J. Besag, P. Green, D. Higdon, and K. Mengersen, “Bayesian computation and stochastic systems,” *Statistical Science*, vol. 10, no. 1, pp. 3–66, 1995.
- [9] N. Metropolis, A. Rosenbluth, M. Rosenbluth, A. Teller, and E. Teller, “Equations of state calculations by fast computing machines,” *J. Chem. Phys.*, vol. 21, pp. 1087–1092, 1953.
- [10] W. Hastings, “Monte Carlo sampling methods using Markov chains and their applications,” *Biometrika*, vol. 57, no. 1, pp. 97–109, 1970.
- [11] C. Geyer and J. Møller, “Simulation procedures and likelihood inference for spatial point processes,” *Scandinavian Journal of Statistics*, vol. 21, pp. 359–373, 1994.
- [12] P. Green, “Reversible jump Markov chain Monte-Carlo computation and Bayesian model determination,” *Biometrika*, vol. 82, no. 4, pp. 711–732, 1995.

- [13] G. Fishman, *Monte Carlo: Concepts, Algorithms and Applications*. New York: Springer-Verlag, 1996.
- [14] J. Besag, “On the statistical analysis of dirty pictures,” *Journal of the Royal Statistical Society, B*, vol. 48, no. 3, pp. 259–302, 1986.
- [15] M. Cowles and B. Carlin, “Markov chain Monte Carlo convergence diagnostics: A comparative review,” *Journal of the American Statistical Association*, vol. 91, no. 434, pp. 883–904, 1996.
- [16] J. Park, D. Metaxas, and L. Axel, “Analysis of left ventricular wall motion based on volumetric deformable models and MRI-SPAMM,” *Medical Image Analysis*, vol. 1, no. 1, pp. 53–71, 1996.